LAMINATED ROCK BEAM DESIGN FOR TUNNEL SUPPORT

D.A.F. Oliveira[1] and L. Paramaguru[2]
[1]Principal Tunnelling/Geotechnical Engineer, Jacobs and Adjunct Principal Fellow, University of Wollongong,
[2] Senior Geotechnical Engineer, Jacobs.

ABSTRACT

The design and construction of semi flat-roofed tunnels, i.e. with a high arch radius to roof span ratio, using a voussoir beam analogy has been proven successful over time. In spite of such a success, the linear arch theory or voussoir beam analogy has always been subjected to a certain level of scepticism due to some of its perceived limitations. Some of the concerns are related to appropriate design methods for the design of rock bolting of multiple beds/laminations in cases where single laminations are deemed unstable upon excavation or while addressing some adverse conditions. This paper investigates the applicability of an analytical solution of the voussoir beam theory for the design of rock bolts in laminated rock beams which has been confirmed with numerical analysis using DEM (Distinct Element Method) analysis. The proposed analysis method can be easily implemented in a spreadsheet to provide rapid assessments though it is considered only one part of the design process with other potential instability mechanisms assessed using other analysis methods.

1 INTRODUCTION

Despite the successful design and construction of semi flat-roofed tunnels over the years in Australia, Canada and the US, the linear arch theory or voussoir beam analogy has always been subjected to a certain level of scepticism due to some of its perceived limitations. According to Diederich and Kaiser (1999), it generated a great deal of controversy when it was first published by Evans (1941), even though the general notion of its successful application traces back to ancient Rome architecture.

A significant portion of the scepticism seems to be related to perceived limitations of the conceptual model and available analytical solutions with respect to:

- The effect of horizontal stress
- Span to lamination/bed thickness ratio
- The presence of adverse geological features
- The effect of a slightly arched roof
- Bolting of multiple beds/laminations in cases where single laminations are unstable upon excavation

It is important to note upfront that there are two primary factors that promote a geological environment amenable to a voussoir beam analogy in tunnel support design: (1) a horizontally bedded rock mass with no low to mid angle jointing cross-cutting the lamination, i.e. a reasonably good quality rock mass, and (2) the existence of favourable horizontal stresses.

This paper investigates the applicability of an analytical solution of the voussoir beam theory through comparison with numerical modelling that focuses on the above limitations. The results illustrate that the voussoir beam analogy can be confidently used in practice when used with reasonable engineering judgment as required in any other design method. It adequately represents the results of more robust numerical solutions such as Discrete Element Method (DEM) when similar governing mechanisms are considered in both models.

2 CONCEPTUAL MODEL AND ANALYTICAL SOLUTION

Rock masses dominated by parallel laminations are often encountered in underground excavations in numerous geological environments. Fayol (1885) noted that, in these cases, the underground strata seemed to separate upon deflection so that each laminated beam transferred its own weight to the abutments rather than loading the laminated beam beneath. This occurred even in the cases where other discontinuities cut across the laminations at steep angles or where reinforcement had been installed. Based on such observations, it was assumed that a compression arch could be generated across the cross-cutting joints and within the beam upon deflection which would then transmit the beam loads to the abutments as illustrated in Figure 1.

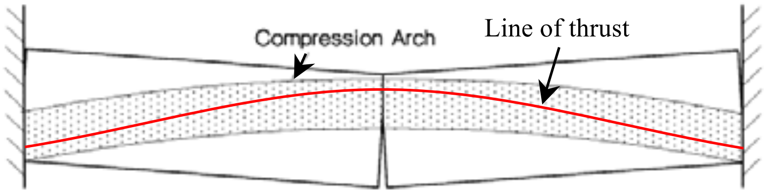

Figure 1: Voussoir beam analog

One of the most recent analytical solutions for analysis of the voussoir beam analogy, and perhaps currently the most widely used, is that proposed by Diederichs and Kaiser (1999). The analytical solution is based on an iterative analysis of beam deflections which is then used for estimates of maximum compressive stress, σ_{max}, developed through the arching mechanism. Such estimates are then adopted to assess factors of safety against four main mechanisms namely rock crushing, sliding or shear at the abutments and a Buckling Limit (BL) Index for the snap-through mechanism. Only one minor adjustment has been made to their original proposal with abutment deflections included according to Asche and Lechner (2003).

A full description of the solution will not be presented here as it can be found in details in Diederichs and Kaiser (1999). However, two main aspects of the original solution are worthwhile highlighting as they will be used later in this paper to investigate the case of multiple laminations: the horizontal stress distribution along the line of thrust within the beam and the geometry of line of thrust itself as depicted in Figure 2.

As noted in Figure 2, Diederichs and Kaiser (1999) assumed a parabolic stress distribution with a quadratic variation at a distance of approximately $S/(2\sqrt{2})$ from the midspan where *s* is the total span of the beam. This point is located where the line of thrust crosses the centreline of the beam and it is reasonable to expect that the entire beam section is under compression and that this stress is constant across the entire beam thickness *T*. As a result, the stress distribution along the line of thrust can be represented by a two-part parabolic curve given by:

$$f(x) = \begin{cases} a_1x^2 + b_1x + c_1 & for\ x \leq \left(\frac{S}{2} - \frac{S}{2\sqrt{2}}\right) \\ a_2x^2 + b_2x + c_2 & for\ x > \left(\frac{S}{2} - \frac{S}{2\sqrt{2}}\right) \end{cases} \tag{1}$$

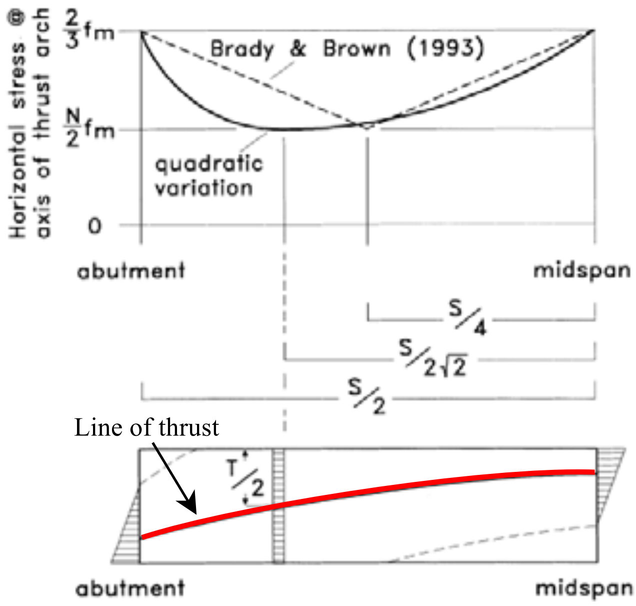

Figure 2: Parabolic compressive stress variation assumed by Diederichs and Kaiser (1999) against Brady and Brown (1993)

where x is the distance along the rock beam and the quadratic parameters may be found from the boundary conditions given in Figure 2 resulting in:

$$a_1 = \frac{\frac{N}{2}f_m - \frac{2}{3}f_m}{-\left(\frac{S}{2} - \frac{S}{2\sqrt{2}}\right)^2} \qquad b_1 = -2a_1\left(\frac{S}{2} - \frac{S}{2\sqrt{2}}\right) \qquad c_1 = \frac{N}{2}f_m + a_1\left(\frac{S}{2} - \frac{S}{2\sqrt{2}}\right)^2$$

$$a_2 = \frac{\frac{N}{2}f_m - \frac{2}{3}f_m}{2\frac{S}{2\sqrt{2}}\left(\frac{S}{2} - \frac{S}{2\sqrt{2}}\right) + \left(\frac{S}{2} - \frac{S}{2\sqrt{2}}\right)^2 - \left(\frac{S}{2}\right)^2} \qquad b_2 = -2a_2\left(\frac{S}{2} - \frac{S}{2\sqrt{2}}\right) \qquad c_2 = \frac{N}{2}f_m + a_2\left(\frac{S}{2} - \frac{S}{2\sqrt{2}}\right)^2$$

where f_m is the maximum compressive stress is given by Diederichs and Kaiser (1999). The geometric position of the line of thrust is given by:

$$y(x) = a_3x^2 + b_3x + c_3 \qquad (2)$$

where the parameters are found by:

$$a_3 = \frac{T - \frac{2NT}{3}}{-\left(\frac{S}{2}\right)^2} \qquad b_3 = -2a_3\left(\frac{S}{2}\right) \qquad c_3 = \left(T - \frac{NT}{3}\right) + a_3\left(\frac{S}{2}\right)^2$$

where T is the lamination thickness and N is the depth ratio for the triangular stress block according to Diederichs and Kaiser (1999). These two equations will play a significant role in the assessment of multiple laminations although not directly and explicitly used in the analysis of a single lamination.

3 NUMERICAL DISCRETE ELEMENT METHOD MODELS

For comparison purposes with a more robust solution, all analyses carried out with the analytical solution are also analysed using a Distinct Element Method (DEM) as encapsulated in UDEC V6.0 (Itasca, 2013). Similar to the numerical models adopted by Diederichs and Kaiser (1999) as part of the development of the analytical solution, the numerical models analysed in this paper use a two-step approach.

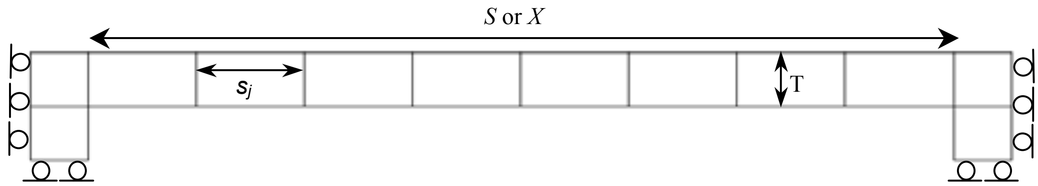

Figure 3: Typical boundary conditions of UDEC models.

The beams are first allowed to deflect elastically while maintaining a non-zero tensile strength within the joints. This initial elastic deflection is assumed equivalent to a gradual excavation mechanism so that some beam deformation occur before the roof is fully excavated and formed. After the initial elastic equilibrium is achieved, the joint tensile strength is set to zero and the beam is allowed to continue deforming until either equilibrium or failure occurs. The joints have no cohesion or dilation but have a frictional strength. One main difference between the model adopted in this paper and that of Diederichs and Kaiser (1999) is that the abutment blocks are given the same deformability parameters of the rock beam instead of a very stiff abutment. Figure 3 presents the typical boundary condition for the UDEC models.

4 EFFECT OF HORIZONTAL STRESS AND SPAN TO BED THICKNESS

The analytical solution for the voussoir beam analogy is bounded by a few limitations. Among others which will be discussed later in this paper, Diederichs and Kaiser (1999) have pointed out that their solution was developed based on span to lamination thickness ratio, $z = S/T$, greater than 10 (see Figure 3). In addition, the impact of horizontal stresses in the rock beam is neglected.

Oliveira and Pells (2014) demonstrated some positive effect of initial horizontal stress on the overall rock beam behaviour by means of DEM modelling which could not be captured by the Diederichs and Kaiser (1999) solution. They suggested that increasing initial horizontal stress causes the beam to behave in a more elastic manner approaching an uncracked rock beam, i.e. with less effect of the cross-cutting joints, and with fixed end conditions at both abutments.

Booker and Best (1990) developed a 1D finite element method which accounted for the effect of horizontal stresses through a "cracked beam" analysis. This method was used for the design of the Sydney Opera House Carpark (Pells *et al*., 1994) and seemed to capture the end effects in a more realistic manner. However, this method involves a finite element solution that is inherently more sophisticated and less used than the Diederichs and Kaiser (1999) solution. As a result, it will not be used or discussed in this paper.

4.1 CONFINEMENT ADJUSTMENT FACTOR

To account for some effect of the initial horizontal stress in the Diederichs and Kaiser (1999) analytical solution, a rock mass confinement adjustment factor is proposed. Although not strictly simulating the effect of initial horizontal stresses on the end conditions of the beam, i.e. not theoretically satisfying the gradual change in bending mechanism from a "free end" towards a "fixed end" condition, it is considered reasonable to assume that confining stresses provide some increase in the rock mass modulus of deformation which would in turn reduce beam deflections.

The proposed adjustment factor is based on Ramamurthy (1995). The modified horizontal rock mass Young's modulus incorporating the effect of confinement, $E_{sb,modified}$, can be estimated based on the relationship:

$$E_{sb,modified} = \frac{E_{sb}}{\left(1-e^{-\alpha\frac{\sigma_{cb}}{\sigma_h}}\right)} \leq 1.5 \ to \ 2.5E_{ib} \quad (3)$$

where σ_{cb} is the block compressive strength at the appropriate scale, α is an empirical exponent to account for the confinement effect, σ_h is the initial horizontal stress and E_{sb} is the horizontal rock mass Young's modulus of a single bed or lamination which is the relevant modulus for the analytical solution. This value may be estimated by:

$$E_{sb} = \frac{E_{ib}k_n s_j}{E_{ib}+k_n s_i} \quad (4)$$

where E_{ib} is the modulus of the "intact" rock block at the appropriate scale, k_n is the normal stiffness of the subvertical joints at a corresponding spacing s_j. In estimating $E_{sb,modified}$, an upper bound value of 1.5 to $2.5E_{ib}$ is proposed for Equation (3). For most of the analyses in this paper, a limiting value of $1.5E_{ib}$ will be adopted.

Based on the database used by Ramamurthy (1995), the exponent α could be said to vary between 0.06 and 0.2 (Figure 4). However, for the effect on a voussoir beam, where the block strength to confining stress ratio, i.e. σ_{cb}/σ_h, is typically low, a value between 0.03 and 0.06 seems to provide reasonable results compared to numerical models as demonstrated as follows. For the low end values of $\alpha = 0.03$, a lower cut-off value of $1.5E_{ib}$ is recommended whereas $2.5E_{ib}$ would be recommended for the high end value of $\alpha = 0.06$.

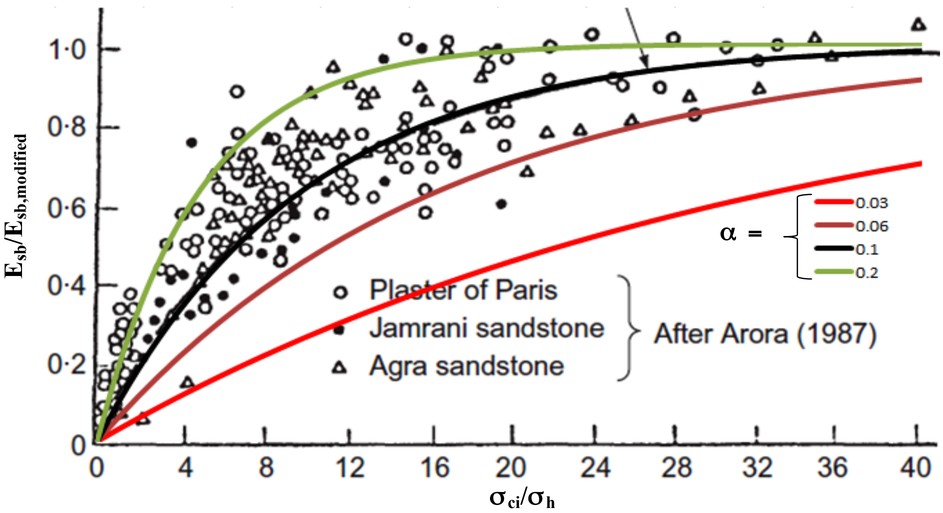

Figure 4: Confinement effect on rock mass modulus (modified from Ramamurthy, 1995).

4.2 COMPARISON WITH DEM RESULTS

The following hypothetical rock design parameters were adopted for the analytical and numerical models:

- Intact block Young's modulus, E_i = 12000 MPa
- Single bed with thickness T = 1.0 m
- Vertical joint spacing, sj = 1.875 m
- Joint normal stiffness, kn = 10000 MPa/m

- Bedding shear stiffness, ks = 10000 MPa/m
- Block scale UCS, σcb = 23 MPa
- Rock unit weight, γ = 26 kN/m3
- Joint/Bedding friction angle, ϕ = 30º
- Bedding dip = 0º

Figure 5 shows the maximum beam deflection against the span to bedding thickness ratio (*z*) for varying horizontal stresses. The modified analytical estimate of beam deflection shows a good agreement with that of the numerical model. For example, the analytical and numerical solutions resulted in a maximum beam deflection of 21 mm for the horizontal stress of σ_h = 0 MPa. It is noted that the analytical and numerical solutions show reasonable agreement for ratios z <10 and the analytical solution could still be applicable for ratios z < 10.

Figure 6 shows the maximum beam deflection against horizontal stress for different *z* ratios. The analytical solution with the proposed confinement effect adjustment seems to provide reasonable agreement with the numerical model, particularly with respect to the overall effect of initial horizontal stresses on the rock beam behaviour. The increase in initial horizontal stress significantly reduces the beam deflection, as previously demonstrated by Oliveira and Pells (2014). For instance, the maximum beam deflections of 21 mm and 8.5 mm were estimated for horizontal stress σ_h = 0 MPa and 4 MPa respectively for a constant span to thickness ratio *z* = 15.

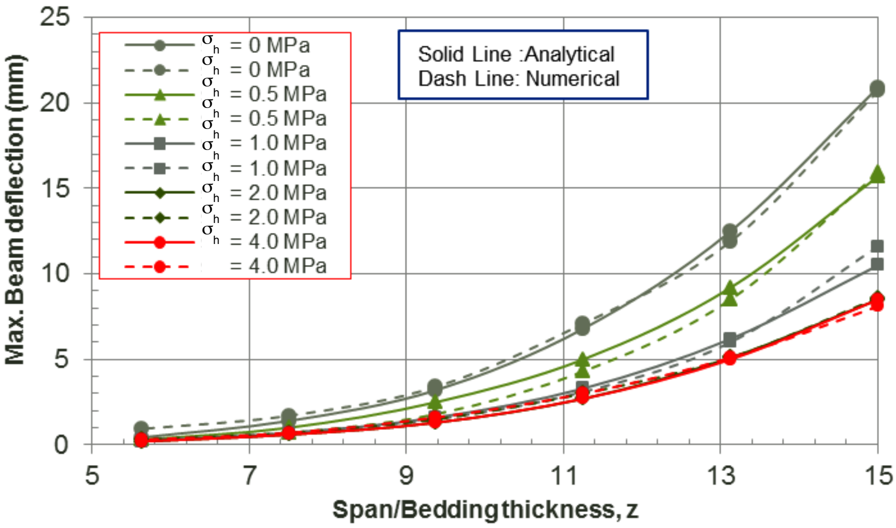

Figure 5: Maximum beam deflection versus span/bed thickness ratio.

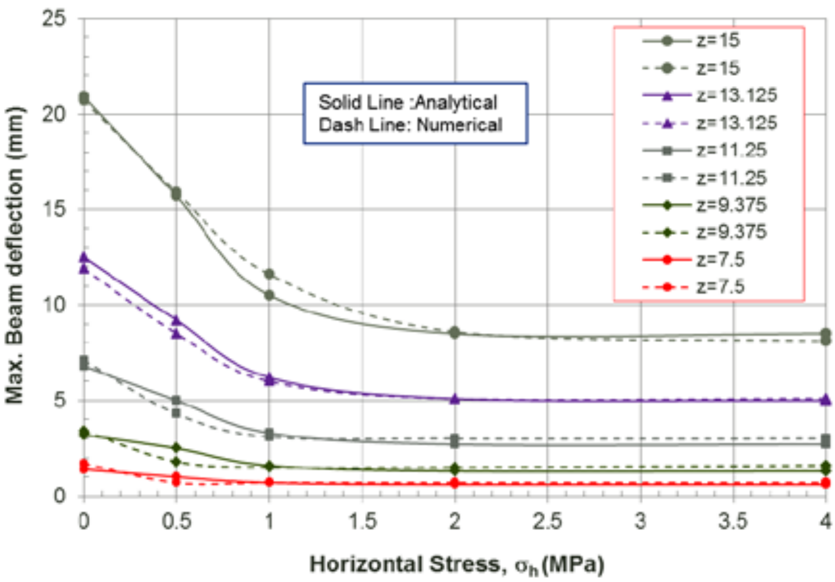

Figure 6: Maximum beam deflection versus horizontal stress for various span-to-bed thickness ratios.

It is important to note that the DEM models require small element size definition to better capture the stress arching and appropriate deflection prediction as pointed out by Oliveira and Pells (2014).

4.2.1 Influence of the confinement factor exponent

The sensitivity of the proposed confinement adjustment factor to higher values of the empirical exponent α has been investigated. Figure 7 shows the variation of maximum beam deflection at σ_h = 0.5 MPa and 1.0 MPa for two values of α but with the same cut-off value of $1.5E_{ib}$. As expected higher values of α reduce the confinement effect in the estimate of the deformation modulus resulting in larger beam deflections. The effect is more pronounced in large span to bed thickness ratios (z > 10). However, as previously discussed a value of α. = 0.03 seems to better represent the numerical model results as show in Figure 5 and Figure 6.

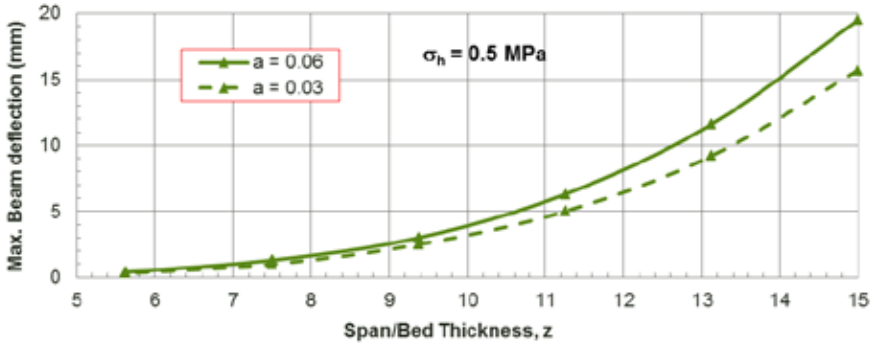

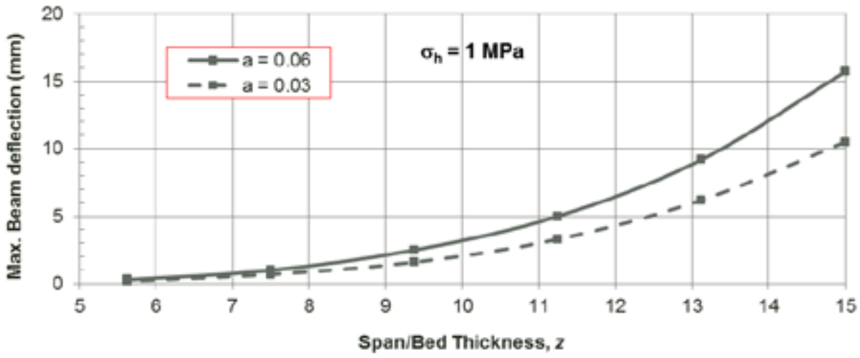

Figure 7: Influence of confinement exponent value on beam deflection.

5 ADVERSE GEOLOGICAL FEATURES IN LAMINATED ROCK BEAM

Like any simplified analysis tool or model, the analytical solution proposed by Diederich and Kaiser (1999) has some limitations. For example, it relies on the assumption that the joints are rough enough to provide frictional resistance under low to moderate confinement (i.e. no slickensides or low friction coating). Translation and sliding failure along joints at the abutments or within the beam is not considered in the iterative solution even though an assessment of factor of safety for such mechanism is possible. In addition, the solution is not considered valid for low to mid angle jointing where the angle between the plane of the cross-cutting discontinuities and the normal to the discontinuities sub-parallel to the excavation plane is more than one third to one half of the effective friction angle of these joints. As a result, Diederichs and Kaiser (1999) did not recommend the use of the voussoir beam method for poor rock masses with low RQD ratings (< 50) and more than three joint sets. The theory also assumes uniform rock compressive strength across the voussoir beam, weak zones located within the compressive regions may adversely affect the stress arching.

Due to the scepticism discussed above, there have been attempts to link some of the above limitations to unacceptable levels of sensitivity for designs based on the voussoir beam analogy. For example, Peck *et al.,* 2013 presented a number of adverse conditions where the voussoir beam analogy would allegedly fail to identify instability. However, besides pointing out significant errors in the sensitivity analyses carried out by Peck *et al*., 2013 Oliveira and Pells (2014) also illustrated that the linear arch analytical model definition can be adjusted in terms of geometry and loading conditions to better capture some adverse conditions as it is also required in more sophisticated DEM models in terms of explicit discretisation.

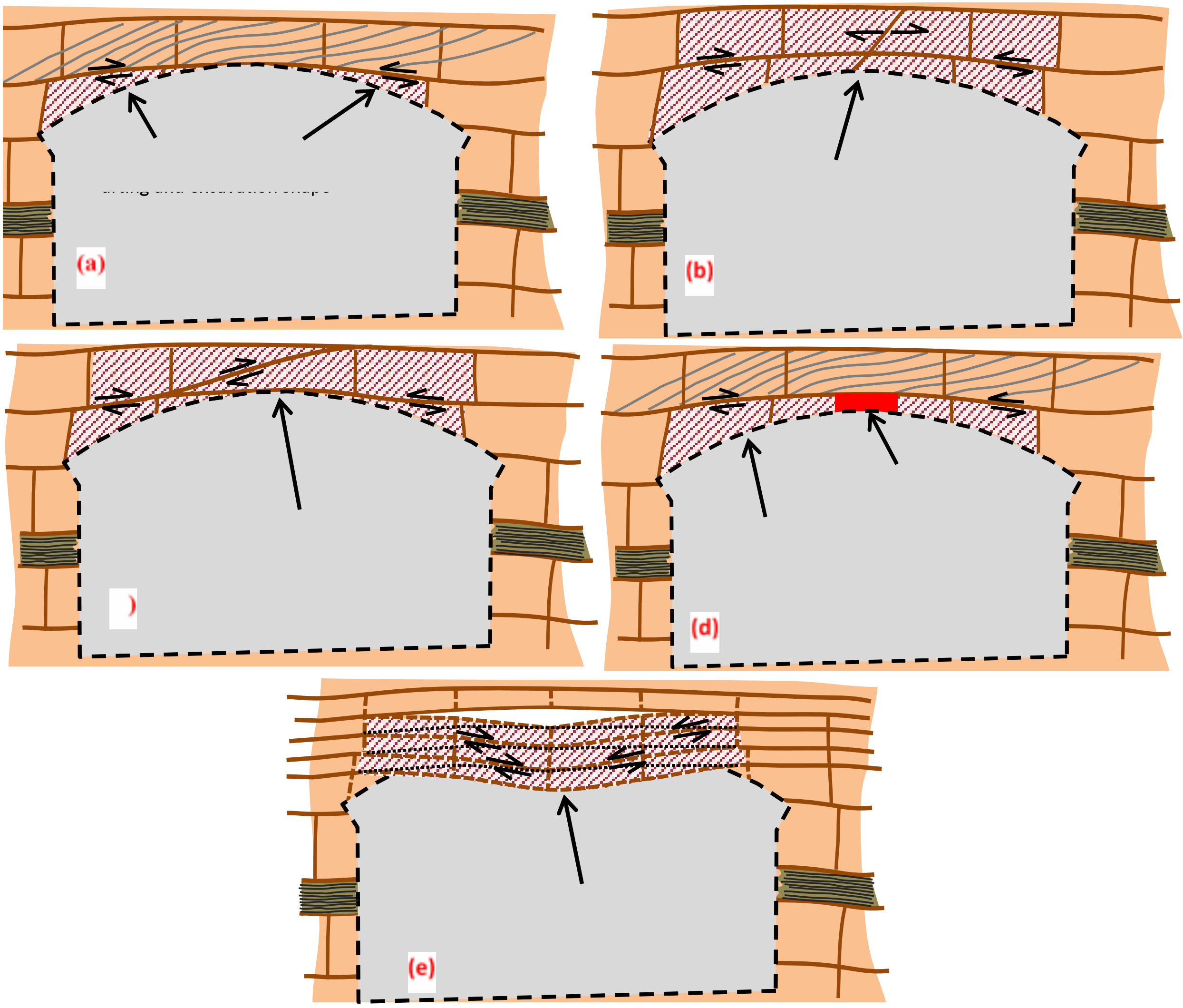

Figure 8: Examples of failure mechanisms affecting the immediate tunnel roof rock beam.

Oliveira and Pells (2014) also highlighted that it is unreasonable to only contemplate design scenarios that are favourable for the voussoir beam analogy and require “perfect knowledge” of a “perfect rock mass”. The analyses must give cognisance to the fundamental importance of rock bolting in providing a robust design against the uncertainties in joint directions that may be expected in strata such as the Hawkesbury Sandstone of Sydney, the Bunter Sandstone of the UK, the Beaufort Series in South Africa and the sandstones at Poatina in Tasmania (Oliveira and Pells, 2014).

Figure 8 presents a few examples of failure mechanisms that need to be addressed as part of the rock bolting design process. Figure 8a shows a classical problem of potentially unstable rock blocks formed by an arched shape in bedded rock. This particular example will be further investigated later in this paper with particular attention to the applicability of the voussoir beam analogy. Mechanisms (a) to (d) of Figure 8 illustrate potentially unstable areas (shaded in red) that would rely on a better performance of upper rock beams. In such cases, the unstable blocks and slabs maybe considered as dead loads for the upper rock beams as a preliminary analysis approach. Figure 8e illustrates a more conventional issue of the voussoir beam analogy for cases where thin laminations would be unstable at a certain span when behaving as single rock beams, therefore requiring to be bolted to the upper roof.

6 BOLTING OF MULTIPLE BEDS/LAMINATIONS

As discussed above rock bolting is of fundamental importance in designs based on a linear arch theory in order to address some of the uncertainties in the rock mass.

The main objective of the rock bolts is to stitch together near horizontal beds of limited and variable thickness to “trick” the rock mass into behaving as an equivalent and appropriately thicker linear arch as depicted in Figure 9. The rock bolts are designed to reinforce the rock mass allowing the development of the compression zone across the bedding partings as illustrated in Figure 9, therefore, controlling shear and slip along the bedding partings that would otherwise result in delamination.

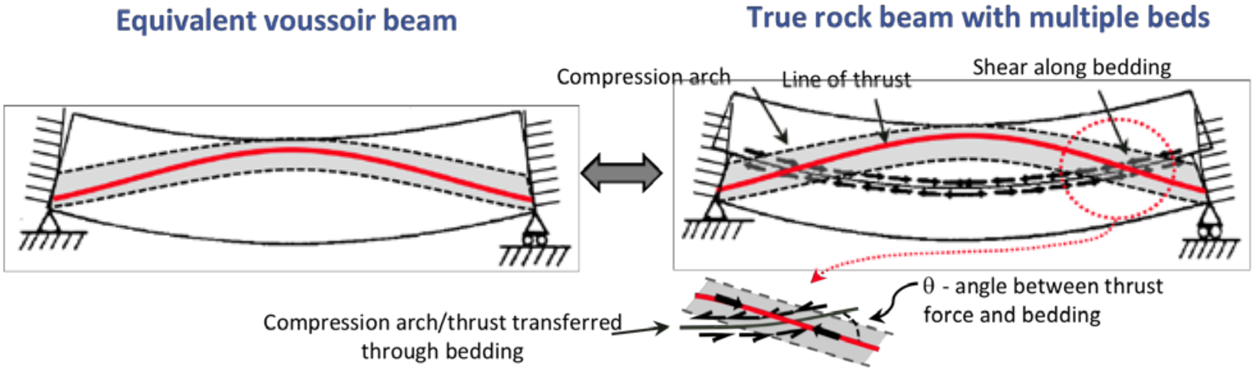

Figure 9: Equivalent rock bolt stitched rock beam (sub-vertical joints not shown for clarity).

The equivalent voussoir beam compressive stresses, *f*, may be estimated using the same methodology described for a single bed with the difference that the new equivalent beam thickness, T_{eq}, corresponds to the sum of the multiple laminations. The development of the compression arch within the equivalent beam will generate both normal and shear forces along the bedding partings which can be estimated by the relationships suggested by Asche and Lechner (2003) given by: Another important aspect in the rock bolt design process is to consider that the mobilisation of the majority of the reinforcement effect generally occurs upon some rock beam deflection and associated shear displacement along the beddings despite some bolt pretension. As a result, in order to assess the mobilised bolt forces, it is necessary to estimate the shear displacements resulting from the shear strain induced by the compression arch within the equivalent beam. The shear displacements are then given by:

$$\tau(x) = f_{(x)} \frac{\sin(2\theta_{(x)})}{1+\cos(2\theta_{(x)})} \tag{5}$$

$$\sigma_N(x) = f_{(x)} \left(\frac{2}{1+\cos(2\theta_{(x)})} - 1 \right) + B_t \tag{6}$$

where *f(x)* is the compressive stresses estimated by Equation (1), B_t is a normal stress induced by any rock bolt pretension before significant rock beam deflections and $\theta(x)$ is the angle between the line of thrust and the horizontal bedding parting which may be found by differentiating Equation (2) resulting in:

$$\theta(x) = atan\left[2\left(\frac{T_{eq} - \frac{2NT_{eq}}{3}}{-\left(\frac{S}{2}\right)^2}\right)\left(x - \frac{S}{2}\right)\right] \tag{7}$$

The available bedding parting shear resistance and consequently excess shear can now be estimated using Equations (5) to (7). The excess shear stress is then used to assess the required rock bolting forces to “trick” the multiple laminations into behaving as an equivalent thicker rock beam and is given by:

$$\tau_e(x) = \tau_{(x)} - \left[\sigma_{N(x)} \tan(\varphi_b) + c_b\right] \tag{8}$$

where ϕ_b and c_b are the friction angle and apparent cohesion of the bedding partings.

An important factor in the assessment of the equivalent bolted voussoir beam behaviour is a reasonable estimate of the effect of the bedding partings on the overall rock beam deflections. The presence of the bedding partings and associated shear displacements upon deflection mean that the rock mass modulus can no longer be estimated by Equation (4) which only accounts for the normal stiffness of the cross-cutting joints. This estimate could be done by a direct assumption of a modulus ratio, E_{sb}/G_{beq}, which often varies between 10 and 20 for transversely isotropic rock masses. However, the authors of this paper have found that the following equation provides a reasonable estimate of the equivalent voussoir beam modulus, E_{beq}:

$$E_{beq} = \frac{E_{sb.modified} E_{sb} k_s T_{sb}}{E_{ib}\left(\frac{E_{sb}}{2(1+\nu)} + k_s T_{sb}\right)} \tag{9}$$

where k_s is the shear stiffness of the bedding partings, ν is the rock mass Poisson’s ratio (typically ν = 0.25), T_{sb} is the average thickness of the individual laminations or bedding parting spacing and all other parameters as previously defined.

Another important aspect in the rock bolt design process is to consider that the mobilisation of the majority of the reinforcement effect generally occurs upon some rock beam deflection and associated shear displacement along the beddings despite some bolt pretension. As a result, in order to assess the mobilised bolt forces, it is necessary to estimate the shear displacements resulting from the shear strain induced by the compression arch within the equivalent beam. The shear displacements are then given by:

$$u_s(x) = \frac{2(1+v)T_{eq}\tau_{(x)}}{E_{beq}} \tag{10}$$

It is important to note that during this design process, an upper bound for the deflection of the rock bolted laminated beam is the deflection of a single lamination. In other words, in general, multiple laminations stitched by rock bolts cannot deflect more than a single bed as this would mean delamination of the beams.

6.1 EXAMPLE OF LAMINATED ROCK BEAM BOLTING DESIGN

An example is provided in this section to illustrate the use of the equations above. The same parameters used in previous comparisons between the analytical solution and DEM models have been used here (Section 4.2). Rock bolts have been initially added at an angle of 90º to horizontal as an attempt to “trick” 3 laminations of 1 m thickness into behaving as a single equivalent 3 m thick rock beam as shown in Figure 10. The analytical solution for rock bolt shear resistance mobilisation adopted is that proposed by Pells (2002) and as modified by Carter (2003).

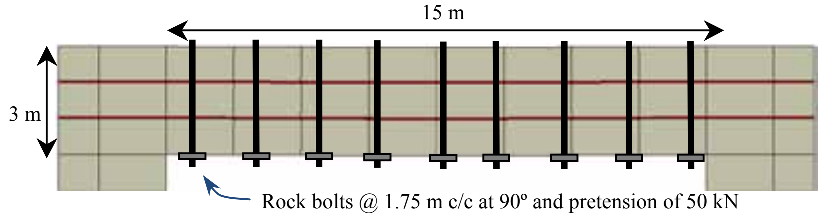

Figure 10: Geometry of composite rock beam and rock bolting.

The results of the analytical analysis using the equations provided above are given in Figure 11 with a predicted deflection of approximately only 5 mm. However, it is evident that the total bolt forces mobilised upon beam deflection (area under black solid line) is significantly less than the excess shear forces (area under the purple solid line) indicating that delamination is possible and the compressive arch as predicted in the equivalent voussoir beam cannot form.

The low mobilization is due to the small deflections resulting in small shear displacements. For example, as anticipated, the largest shear displacement predicted in the analysis is near the abutment with a value approximately 0.75 mm. It can be observed on the right hand plot of Figure 11 that a joint shear displacement of 0.75 mm would only mobilise a total shear force of approximately 70 kN which divided by the tributary area of 1.53 m^2 (one bolt spacing longitudinally and half bolt spacing transversely near the abutment) only provides an additional shear resistance of approximately 46 kPa as shown on the left hand side plot.

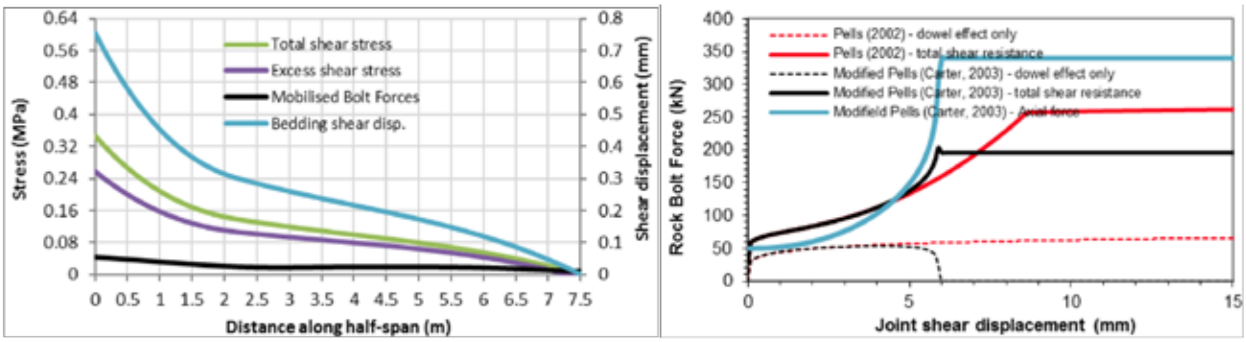

Figure 11: Analytical results for 3 m thick beam with σ_h = 0 MPa, bolts at 90º and k_s = 10000 MPa/m.

As an attempt to improve the performance of the stitched laminated beam, the bolts are now considered to be installed at a 70º angle to horizontal as shown in Figure 12. At such an angle, the rock bolts are likely to intersect the sub-vertical joints and consequently generate additional axial forces. The bolts may also intersect multiple beddings within the voussoir compression arch length at slightly different locations (Figure 17). For simplicity, to account for the bolts crossing multiple beds, the total mobilised bolt force can be multiplied by MAX[$N.(n_b$-1),1] where N is the depth ratio for the triangular stress block and n_b the number of beds. In addition, assuming that the rock bolts intersect the sub-vertical joint near the bolt-bedding plane intersection, it can be considered reasonable to assume that this additional axial force is similar to that developed within a bedding plane. This has been confirmed in the numerical models (Figure 17). The latter additional axial forces can then be converted to additional normal forces and consequently frictional resistance.

The results are provided in Figure 13. The rock beam behaviour remains essentially the same as the stiffness provided by the rock bolts added to that of the bedding has only a small influence on the beam deflections. However, the rate of rock bolt forces mobilisation is significantly higher which results in more rock bolt forces mobilised for the same shear displacement. For example, full bolt shear resistance is mobilised at approximately 1.2 mm. In addition, due to the rock bolts intersecting the sub-vertical joints, additional axial forces were included in the shear resistance as discussed above. However, the mobilised bolt shear forces/stresses are below the excess bedding shear stress which means that the compressive arch in the equivalent beam cannot develop.

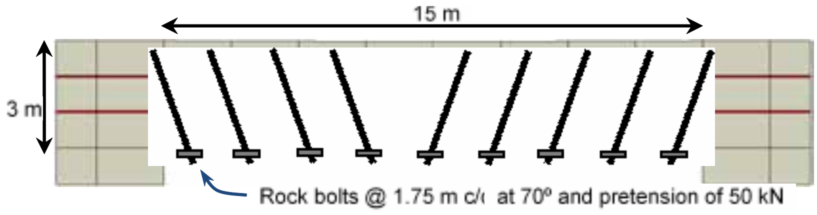

Figure 12: New rock bolting geometry.

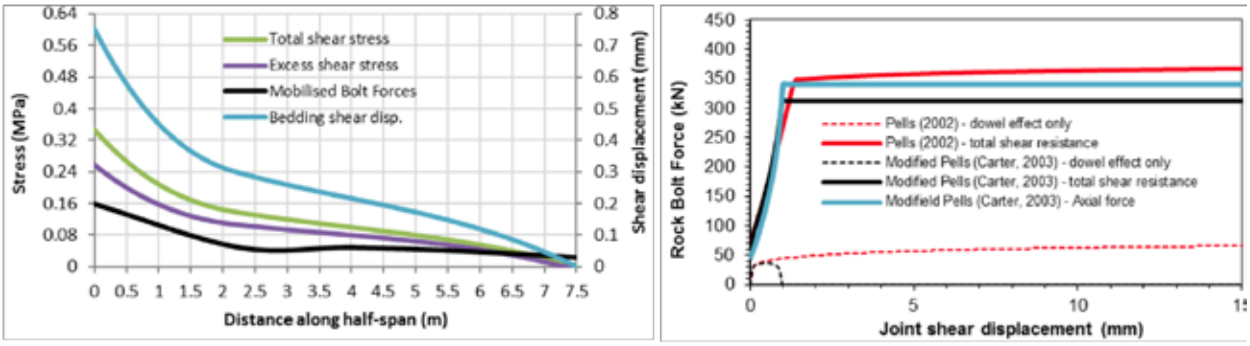

Figure 13: Analytical results for 3 m thick beam with σ_h = 0 MPa, bolts at 70° and k_s = 10000 MPa/m.

One could ask what would be the consequences of the compressive arch not being formed in the previous analysis. As depicted in Figure 9, the compressive arch generates both shear and normal forces across on the bedding parting. If such forces are not resisted by the combined bedding and rock bolting shear resistance, plastic shear displacement or slippage along the bedding parting takes place as illustrated by the red arrows in Figure 14. Such plastic shear displacements induce further deflection of the rock beam which in turn could mobilise additional rock bolt shear resistance. A simplified approach to capture such a mechanism is to artificially and iteratively reduce the bedding parting shear stiffness which in turn reduces the equivalent thicker voussoir beam modulus (Equation 9). This process, as illustrated in Figure 14, is carried until there is equilibrium between the excess shear forces and the rock bolt mobilised forces or until the beam behaves as single laminations, if stable, or become unstable.

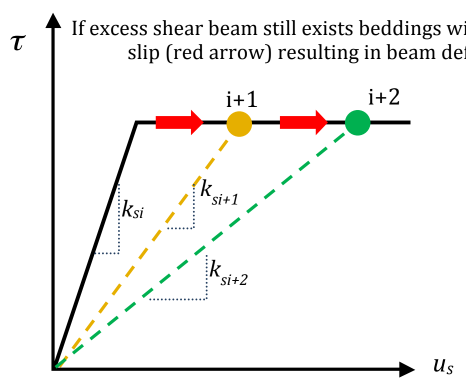

Figure 14: Proposed iterative approach for rock bolt mobilisation upon plastic shear displacements.

Figure 15 presents the results of the previous analysis adopting the proposed iterative approach. Equilibrium between excess shear force and rock bolt mobilised shear forces is reached when the bedding shear stiffness is reduced to approximately $k_s = 1500$ MPa/m with a corresponding beam deflection of approximately 11 mm. The rock bolt mobilisation curve is the same is that presented in Figure 13.

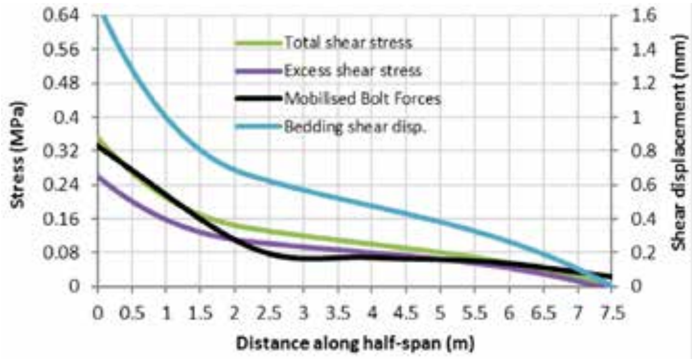

Figure 15: Analytical results for 3 m thick beam with $\sigma_h = 0$ MPa, bolts at 70º and $k_s = 1500$ MPa/m.

A comparison between the analytical approach proposed above and DEM models is presented in Figure 16. A single bed analysis is presented for reference. Like the analytical solution, the DEM model also indicates that the bolts do not mobilise enough shear resistance for the development of the thicker rock beam if installed at a 90º angle. The beam behaviour is compatible with that predicted by the analytical approach and similar to that of a single lamination which is the limiting deflection for a stable beam.

Figure 17 shows the stress arching in the bolt stitched 3 m beam with rock bolts installed at 70º, $\sigma_h = 0$ MPa and $k_s = 10000$ MPa/m. The resulting deflection is approximately 11 mm, similar to the analytical prediction. The reinforcement effect of the rock bolts and tensile zones (or zero stress) developed in the beam are evident through the stress tensors in red colour, and consistent with the conceptual model discussed above. The effect of the rock bolts on the sub-vertical joints can also be observed.

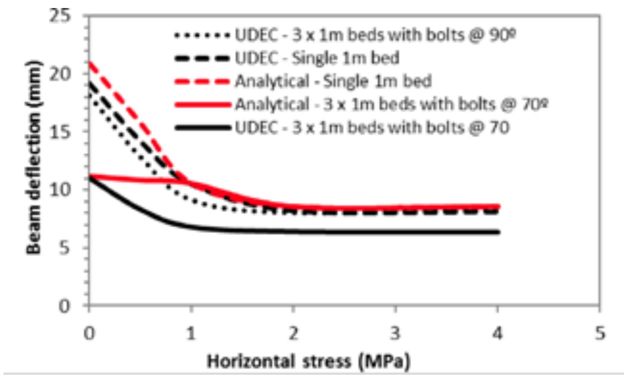

Figure 16: Analytical versus UDEC models for 3 m thick beam with bolts at 90º and 70º.

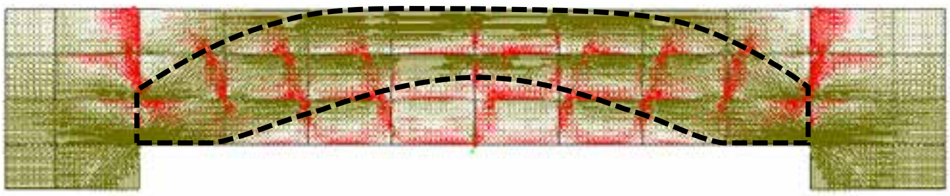

Figure 17: Stress tensor illustrating arching in DEM model - 3 m thick beam, bolts at 70º, $\sigma_h = 0$ MPa and $k_s = 10000$ MPa/m.

In summary, both analytical and UDEC models show similar trends in all cases analysed despite the small differences in deflection (1-4 mm) likely resulting from the simplified assumptions on the effect of initial horizontal stresses, equivalent beam modulus and also the differences in how the rock bolts are modelled in both solutions. As a result, the analytical approach is considered to provide a reasonably satisfactory prediction of the overall performance of the bolted laminated rock beam.

6.2 A BRIEF NOTE ON SURCHARGE LOADINGS FOR VOUSSOIR BEAM ANALYSIS

In the case of single laminations of constant thickness, where there is reasonable rock cover capable of promoting a stress arching, the beams are generally considered to separate or delaminate upon deflection so that each rock beam transfers its own weight to the abutments without loading the laminated beam beneath. However, it is necessary to account for the fact that not all rock beds have the same thickness. Thinner laminations located higher in the roof would tend to have higher deflection imposing some loading on the lower laminated beams. This becomes even more evident in the case of multiple laminations stitched by rock bolting where the increase in the "lower beam flexural stiffness" constrains the deflection of the upper laminations resulting in some surcharge loading on the bolted rock beam. As a result, it is generally needed to consider some loading in the design of laminated rock beam bolting.

Similar observation was also made by Obert and Duvall (1967) who pointed out that the behaviour of rock beams in a tunnel roof is dependent on their relative flexural stiffness. For cases where the upper beam is stiffer than the lower beam, these two beams would behave independently and delaminate from each other (Figure 18a). Where the lower beam is stiffer, the upper beam would load the lower beam and conversely the lower beam would support the upper beam (Figure 18b).

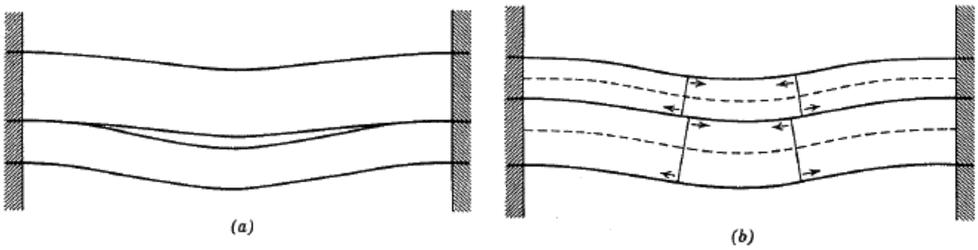

Figure 18: Behaviour of multiple beams with fixed end (after Obert and Duvall, 1967).

Based on a number of assumptions but mainly that the beams would have the same deflection over their entire length, Obert and Duvall (1967) suggested that for a simplified two beam system the additional load to be added on the lower beam and subtracted from the upper beam, could be estimated by:

$$\Delta q = \frac{w_l E_u I_u - w_u E_l I_l}{E_u I_u + E_l I_l} \tag{11}$$

where the subscripts "*u*" and "*l*" refer to the upper and lower beams respectively, *w* is the beam self-weight as a uniformly distributed load, *I* is the second moment of area of the beam and *E* the deformation modulus. Similar estimates could be made for an assumed number of beds. However, Obert and Duvall (1967) have not considered the effect of sub-vertical cross-cutting joints and how it would affect the values of "*l*", i.e. the voussoir analogy. In addition, the designer would still have to assume a certain number of beams in the roof.

The authors of this paper have found that, as a first guess, a parabolic surcharge equivalent to an overburden of approximately 0.25 times the span of the beam provides a reasonable and safe first estimate when comparing to DEM models with enough rock cover. It is important to note that upon increasing deflections, one could consider that such a surcharge reduces up to a deflection corresponding to full delamination where the single beds are assessed stable and sustaining their own weight. If the material above the rock beam is considered unable to arch, this load would remain constant upon deflection. In addition, this loading percentage could increase to 1 times the span above the rock beam for a tunnel cover in soft ground, i.e. soil.

6.3 DIFFERENCES BETWEEN ROCK BOLT DESIGN APPROACHES IN LAMINATED BEAMS

It is important to note the difference in the underlying philosophy of the design approach adopted in this paper and that proposed by Bertuzzi and Pells (2002). Bertuzzi and Pells (2002) philosophy is to use the displacements derived from a jointed rock mass analysis to design a rock bolt reinforcement that provides greater capacity than the stresses derived from an elastic equivalent continuum analysis. The use of the continuum analysis was justified by Bertuzzi and Pells (2002) as means to take advantage of the high *in situ* stresses that were ignored in the jointed beam analysis.

The current approach focuses on satisfying the development of the compressive arch of the equivalent thicker voussoir beam analysis while embeddding the effect of high initial horitonal stresses in the jointed beam analysis, though in a simplified manner. The rock bolt reinforcement is designed to provide the necessary capacity to overcome the excess shear stresses in the bedding partings. For the purpose of rock bolting design in laminated beams, equivalent elastic continuum analysis are not strictly required in the current proposal.

However it would still be necessary to assess the stress redistribution around the excavation and associated failure mechanisms suchs as lamination buckling when behaving as column (Euler buckling), spalling and others. In doing so, an equivalent elastic continuum analysis could be carried out, particularly considering a transversely isotropic behaviour where elastic anisotropy related to the differences in vertical and horizontal modulus and a ratio of E/G = 10 to 20 can be captured. This can be easily achieved using programs such as Examine2D from Rocscience. The results of this equivalent continuum analysis can then be used as an alternative check. The designer may verify the total shear stress induced by the tunnel excavation and the normal stresses acting on the bedding partings at a certain depth into the roof, say 0.5 m to 1 m, therefore being able to estimate the excess shear stress. The rock bolts assessed with the current voussoir beam analogy approach can then be verified against the excess shear stress developed in the equivalent continuum analysis.

In doing both verifications, the designer will target two primary objectives: (1) satisfy the formation of the compressive arch in the voussoir beam analogy, and (2) attempt to maintain the roof (laminated rock beam) behaviour as close to an elastic behaviour as practically possible where deflections are controlled to acceptable levels.

7 EFFECT OF A SLIGHTLY ARCHED ROOF

Although the voussoir beam analogy has been successfully used in the design and construction of a number of tunnels with flat to semi-flat roofs, with high arch radius to roof span ratio, there is certain scepticism of its application in slightly arched-roof tunnels. This question becomes even more relevant with the recent requirements for water resisting linings on road tunnels in NSW where some arch is required to allow the secondary lining, which is not structurally connected to the rock bolts, to span the water loads to the tunnel abutments. As a result, this section will investigate the applicability of the voussoir beam analogy to arched tunnels based on the initial assumption that it is the bedded nature of the rock that dictates its behaviour.

As depicted in the failure mechanism of Figure 8a, one of the negative effects of an arched profile in a horizontally bedded rock is the potential formation of unstable side wedges that would tend to fall-out and “square out” the excavation. These unstable wedges need to be bolted to an upper rock beam which will now have two potential behaviours: (1) work as single beam that is loaded by the unstable wedge or (2) work as an equivalent voussoir beam with a portion that is removed (see grey shade in Figure 19).

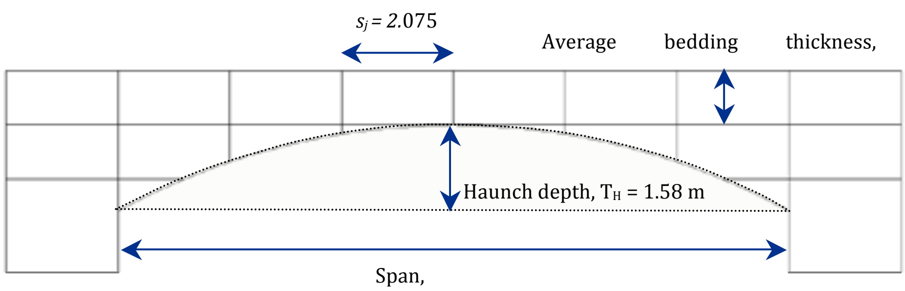

Figure 19: Geometry and boundary conditions for case 1.

The example given in Figure 19 will be analysed using both analytical and numerical approaches to in order to investigate the effect of the arch on the voussoir beam behaviour. In this case a rise to span ratio of 0.127 m/m has been adopted resulting in a haunch depth of approximately T_H = 1.58 m. The following parameters have also been adopted:

- Intact block modulus, E_i = 4000 MPa
- Bedding thickness, b = 1.0 m
- Vertical joint spacing, s_j = 2.075 m
- Joint normal stiffness, k_n = 8000 MPa/m
- Bedding shear stiffness, k_s = 800 MPa/m
- Intact block UCS, σ_{ci} = 12 MPa
- Rock unit weight, γ = 26 kN/m3
- Joint friction angle, ϕ = 40º

As an initial assumption, the potentially unstable wedges are considered simply as dead loads applied to the upper 1 m thick rock beam. This load is applied as an equivalent distributed load that applies the same moment at the abutment contact with the rock beam (Figure 20). This is conversion is consistent with the solution of the voussoir beam targeting a compensated moment generated at the abutment due to self-weight of the beam with a resisting moment as the beam deflects (Diederichs and Kaiser, 1999).

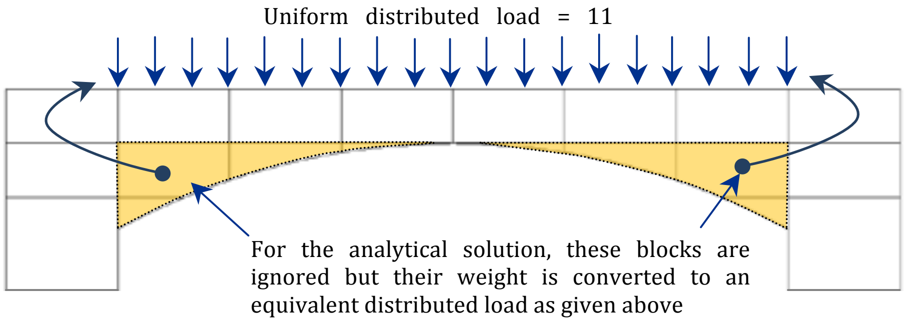

Figure 20: Initial assumption for analytical model case 1.

A second assumption is to consider that the arched voussoir beam still behaves as one laminated beam. However, as suggested by Asche and Lechner (2003), two adjustments are necessary in the voussoir algorithm. The first is that the effective density can be reduced to take account of the removal of rock mid-span, i.e. the beam does not have a constant T_{eq}. Secondly, in removing the rock, the average stress must rise in the arch, and the elastic shortening which is calculated in the algorithm increases slightly. As an adjustment factor Asche and Lechner (2003) suggested that the effective density could be estimated by:

$$\gamma_{arch} = \gamma \frac{T_{eq} - T_H}{T_{eq}} \tag{12}$$

Assuming that some material has been removed from the beam (Figure 19), Asche and Lechner (2003) suggested that the lowest stress, used to calculate the average stress, must be higher than that presented by Diederichs and Kaiser (1999) as depicted in Figure 2. As a result, assuming that the force is unchanged, the new lowest stress could be estimated by;

$$f_{low} = \frac{N}{2} f_m \frac{T_{eq}}{T_{eq} - T_H} \tag{13}$$

It is important to note that the above corrections are made within the iterative approach proposed by Diederich and Kaiser (1999). This means that the final value of f_m found with the iterative approach is already the corrected value and no further adjustments need to be made in Equation (1).

Figure 21 shows the maximum beam deflection against the horizontal stress for the arched tunnel roof analysis. The differences in deflections may be the result of two main assumptions: (1) the simplified approach adopted to account for the effect of the initial horizontal stress and (2) the estimates of rock beam deformation modulus are based on average spacing of the discontinuities, i.e. bedding partings and joints, which are no longer constant in the case analysed. The discrete discontinuities better captured in the DEM model result in stiffer rock beams and therefore with smaller deflections. Nevertheless, the maximum deflections predicted are considered to show a satisfactory agreement with similar trends. The analytical solution seems to over predict the beam deflections compared to that of the numerical solution due to the factors discussed previously. It should be noted that one rock bolt per rock wedge have been introduced at 90º angle to provide stability to the blocks underneath the beam and these have affected to the deformation of the beam. The analytical solution is not sensitive to initial horizontal stresses greater than 0.5 MPa whereas the numerical model still indicates some minor reduction in deflections.

A second case was analysed considering that the tunnel roof arch creates an undercut on the first "continuous" rock beam in the roof, leaving a beam thickness of only 0.75 m as depicted in Figure 22. Similar to "Case 1", as an initial assumption, the potentially unstable wedges are considered as an equivalent distributed load applied to the upper rock beam with a corresponding value of q = 4 kPa.

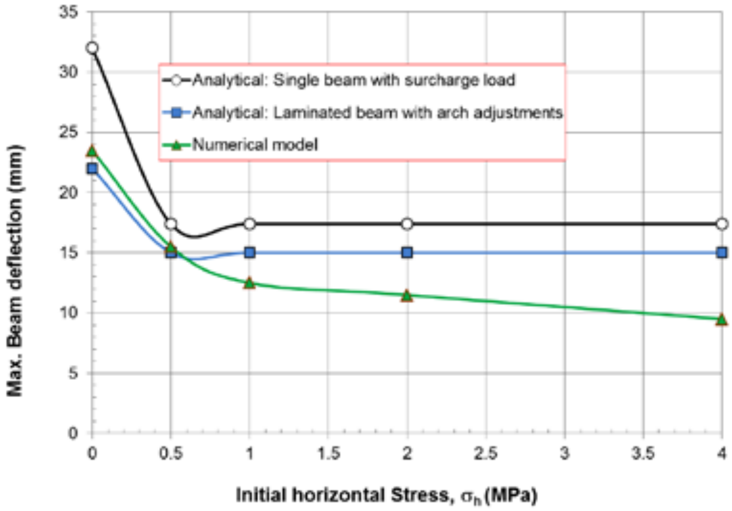

Figure 21: Maximum beam deflection for arched tunnel roof - case 1.

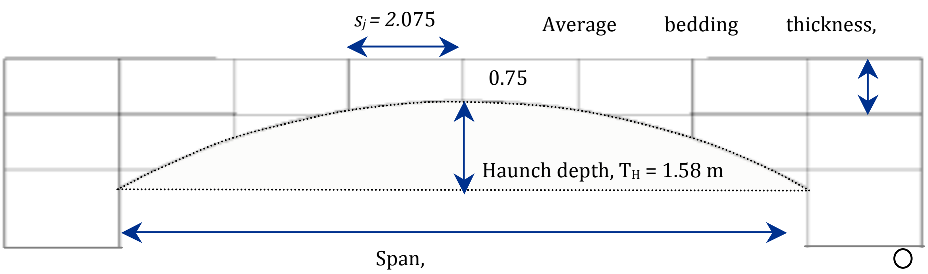

Figure 22: Geometry and boundary conditions for case 2.

Figure 23 shows the maximum beam deflection against the horizontal stress for arched tunnel shown in Figure 22. Similar to the previous case, the maximum predicted deflections are in reasonable agreement with the DEM model. The lower deflections compared to "Case 1" are a direct result of the lower equivalent surcharge applied by the smaller wedges (4 kPa compared to 11 kPa in Case 1).

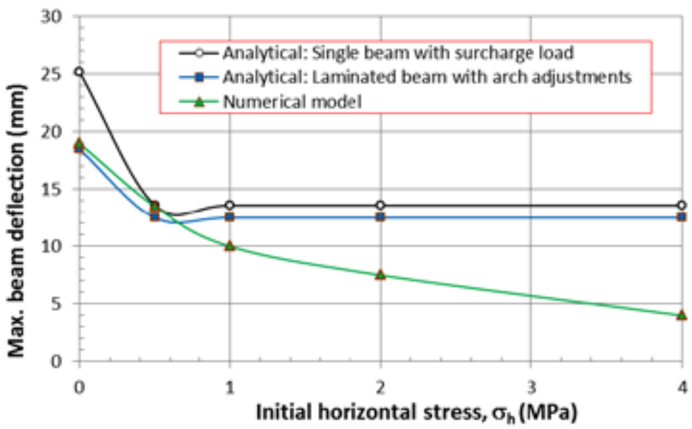

Figure 23: Maximum beam deflection for arched tunnel roof - case 2.

Again, the differences in deflections may be explained by the simplified approaches adopted for both horizontal stresses and rock bolt mobilisation. The combined cut-off values of $1.5E_{ib}$ and $\alpha = 0.03$ previously adopted for the effect of initial horizontal stresses have a particular effect which can be observed in the shape of the curve of Figure 21 and Figure 23. To investigate this effect, additional analyses were carried out assuming an increased cut-off value of $2.5E_{ib}$ with $\alpha = 0.06$. The results are shown in Figure 24. As expected, there is a better agreement with the DEM predictions, indicating that for low stiffness rock beams such as those with low intact block modulus or with an undercut arch, higher values of α and effect cut-off value may be more appropriate, i.e. $\alpha = 0.06$ and $2.5E_{ib}$ respectively.

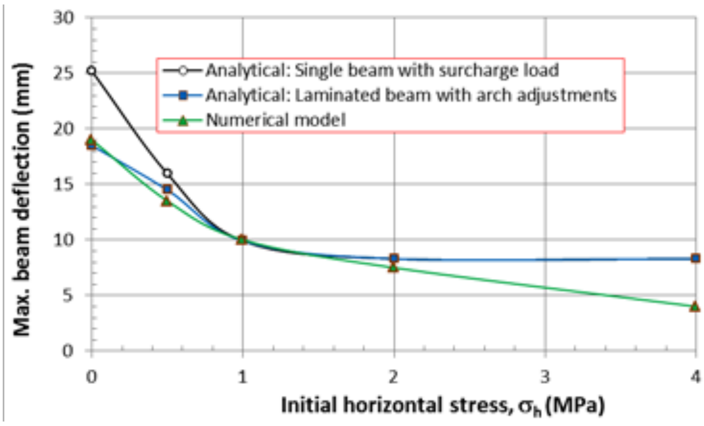

Figure 24: Maximum beam deflection for arched tunnel roof with modified confinement factors- case 2.

8 CONCLUSIONS

A significant portion of the scepticism for the use of a voussoir beam analogy seems to be related to the perceived limitations of the conceptual model and available analytical solutions with respect to the effect of horizontal stress, span to lamination/bed thickness ratio, the presence of adverse geological features, the effect of a slightly arched roof. In addition, there is also some concern on appropriate design methods for the design of rock bolting of multiple beds/laminations in cases where single laminations are deemed unstable upon excavation.

The examples adopted in this paper sought to demonstrate that the effect of initial horizontal stresses may be taken into account through a simplified approach though not strictly capturing the theoretical mechanism. They also demonstrated that the solution still provides acceptable results for span to lamination thickness ratio less than 10, limit suggested by Diederich and Kaiser (1999). The effect of an undercut arch was also investigated with satisfactory results found with the analytical solution.

The primary objective of the rock bolting design approach adopted in this paper is to promote the development of the compressive arch within the "stitched" equivalent rock beam. This is achieved by assessing the excess shear forces developed within the equivalent beam and comparing with the mobilised rock bolt forces estimated through methods such as those presented by Pells (2002).

As a result, this paper illustrates with several examples and discussion of the underlying assumptions that an analytical solution of the voussoir beam analogy can be successfully used as a simplified tool for the assessment of roof support in strongly bedded rocks where jointing orientations and horizontal stress conditions provide a favourable environment. It is not suggested as the only means of assessment, particularly considering the significant advances in discontinuum rock mass numerical modelling. However, the voussoir analogy provides the designers with a simple tool that can be programmed into a spreadsheet and used to test scenarios and conditions in a quick manner, providing some insight into expected behaviours.

9 REFERENCES

Asche, H.R. and Lechner, M.K. (2003). Design for the Cross City Tunnel, Sydney. Proceedings of the RETC. Seattle. pp. 122-139.

Bertuzzi, R and Pells, P J N (2002). Design of rock bolt and shotcrete support of tunnel roofs in Sydney sandstone. Australian Geomechanics, 37(3).

Booker and Best (1990). Coffey internal communication.

Carter, J. (2003). Pells analysis of the shear behaviour of a reinforced rock joint. Report by Advanced Geomechanics, Sydney University,

Diederichs, M S and Kaiser P K. (1999): Stability Guidelines for Excavations in Laminated Ground - The Voussoir Analogue Revisited, Int. J. Rock Mech. & Min. Sci.; 36, pp 97-118.

Evans W H. (1941). The strength of undermined strata. Trans. Inst. Min. Metall., 50:475-500.

Fayol, M. (1885). "Sur les movements de terrain provoques par l'exploitation des mines," Bulletin de la Société de l'industrie Minerale, 2nd Series, Vol. 14, pp. 818.

Itasca (2014). Universal Distinct Element Code User's Guide.

Oliveira D. and Pells, P. (2014) Revisiting the applicability of voussoir beam theory for tunnel design in Sydney. Australian Geomechanics Vol 49(3), pp 29-44, September

Pells, P J N, Best, R J, and Poulos, H G (1994). Design of roof support of the Sydney Opera House underground parking station. Tunnelling and Underground Space Technology, Vol 9, No 2, pp201-207.

Pells, P. J. N. (2002). Developments in the design of tunnels and caverns in the Triassic rocks of the Sydney region. International Journal of Rock Mechanics and Mining Sciences 39: 569-587

Peck, W A, Sainsbury, D P and Lee, M.F (2013). The importance of geology and roof shape on the stability of shallow caverns. Australian Geomechanics, 48(3).

Ramamurthy, T. (1995). Strength and modulus response of anisotropic rocks. In Comprehensive rock engineering (ed. J. A. Hudson), Oxford, Pergamon Press, Vol. 1, pp. 313–329.